

Podoplanin expression in tumor-free resection margins of oral squamous cell carcinomas: an immunohistochemical and fractal analysis study

C. Margaritescu¹, M. Raica², D. Pirici³, C. Simionescu¹, L. Mogoanta³, A.C. Stinga¹, A.S. Stinga¹ and D. Ribatti⁴

¹Department of Pathology, University of Medicine and Pharmacy Craiova, Romania, ²Department of Histology, University of Medicine and Pharmacy "Victor Babes", Timisoara, Romania, ³Department of Histology, University of Medicine and Pharmacy Craiova, Romania and ⁴Department of Human Anatomy and Histology, University of Bari Medical School, Bari, Italy

Summary. Podoplanin is involved in tumorigenesis and cancer progression in head and neck malignancies and its expression is not restricted to lymphatic vessel endothelium. The aim of this study was to establish podoplanin expression in the tumor-free resection margins of oral squamous cell carcinomas (OSCCs) and to evaluate the geometric complexity of the lymphatic vessels in oral mucosa by utilizing fractal analysis.

As concerns the podoplanin expression in noncancerous tissue, forty tumor-free resection margins from OSCCs were investigated utilizing immunohistochemistry for D2-40 antibody and image densitometry analysis. Podoplanin expression was extremely low in basal cells, especially in resection margins of OSCCs developed in the lower lip regions. However, a highly variable D2-40 expression in tumor-free resection margins associated with hyperplastic or dysplastic lesions was identified. Moreover, podoplanin expression also extended to the basal layer of the lower lip skin appendages, the myoepithelial cells of acini and ducts of minor salivary glands, and other structures from the oral cavity.

As concerns the study of the density and complexity of oral lymphatic vessels architecture by means of immunohistochemistry (D2-40, CD31 and Ki-67 antibodies) and fractal analysis, we demonstrated that in normal oral mucosa the geometry of the lymphatic vessels was less complex at the level of the lower lip compared to the anterior part of the oral floor mucosa or the tongue. A comparative analysis between the normal and pathological aspects revealed statistically significant

differences between the fractal dimension (FD) of the vessels' outline, especially in the tongue. Fractal analysis proved an increasing lymphatic network complexity from normal to premalignant oral mucosal lesions, providing additional prognostic information in oral malignant tumors.

Key words: Fractal analysis, Lymphatic vessel, Oral mucosa, Podoplanin

Introduction

Human podoplanin is a 38 kDa type-1 transmembrane glycoprotein encoded by one of the highest expressed lymphatic-specific genes in cultured human lymphatic endothelial cells (Hunyady et al., 1996) and is a key factor involved in the control of the development of lymphatic progenitor cells from embryonic veins (Hong et al., 2002). Although the physiological function of podoplanin is still unknown, numerous studies proved its involvement in cancer cell migration, invasion, metastasis, malignant progression (Martin-Villar et al., 2006; Wicki et al., 2006; Wicki and Christofori, 2007), platelet aggregation (Kaneko et al., 2006), tissue development and repair (Nose et al., 1990; Gandarillas et al., 1997).

In normal tissues, podoplanin is expressed in the apical surface of rat alveolar type I cells (Rishi et al., 1995), in lymphatic endothelium (Breiteneder-Geleff et al., 1999), in kidney podocytes (Breiteneder-Geleff et al., 1999), in skeletal muscle, placenta, lung and heart (Martin-Villar et al., 2005), in the myofibroblasts of the breast and salivary glands, in osteoblasts and mesothelial cells (Ordonez, 2006), and in basal layer of the human epidermis (Schacht et al., 2005).

The aim of this study was to evaluate the expression of podoplanin in oral mucosa bioptic specimens in lower lip, tongue and oral floor obtained from the tumor-free resection margins of oral squamous cell carcinomas (OSCCs) by means of a monoclonal antibody raised against a fixation resistant epitope on podoplanin (D2-40) (Schacht et al., 2005) and to study the density and geometry of the oral lymphatic vessels by means of fractal analysis.

Materials and methods

Patients and tissue specimens

Forty tumor-free resection margins bioptic specimens obtained from oral squamous cell carcinomas (OSCCs) were selected from the archive of the Department of Pathology of the Emergency Hospital N.1 of Craiova. The clinico-pathological data are summarized in Table 1.

This study was focused on the analysis of podoplanin expression at the level of the resection margins with normal and preneoplastic aspects confirmed by microscopic analysis of OSCCs specimens, not invaded by tumor cells at a distance of around 1 cm from the tumor. Moreover, podoplanin expression was also analyzed also at the level of the tumor. The study was approved by the local ethical committee, and written informed consent was obtained from all the patients.

Tissue processing and immunohistochemistry

Five-micrometer thick sections were deparaffinized in xylene and rehydrated through a graded alcohol series, and subjected to single and double immunohistochemistry using the monoclonal antibody

anti-D2-40 (Dako, Redox Bucharest, Romania), Ki-67 (Thermo Fisher Scientific Inc., Cheminkpress, Craiova, Romania) and a polyclonal antibody anti-CD31 (Abcam, Cheminkpress, Craiova, Romania).

Enzymatic immunohistochemistry

After the antigen retrieval step, sections were incubated in 3% hydrogen peroxide in PBS for 15 min to block endogenous peroxidase activity. Sections were then processed according to the peroxidase-conjugated polymer backbone technique (Dako), as follows: i) the unspecific antibody-binding sites were blocked utilizing the blocking reagent; ii) the sections were incubated with the D2-40 antibody diluted 1:200 in 1% bovine serum albumin in PBS and 0.05% Tween, at 4°C overnight, followed by signal development using the EnVision™ Detection Systems Peroxidase/DAB, Rabbit/Mouse kit according to the manufacturer's protocol. Antibody detection was performed with 3,3'-Diaminobenzidine (DAB) chromogen substrate solution (Vector Laboratories, Cheminkpress, Craiova, Romania). For double detections (D2-40/CD31), species-specific secondaries conjugated with alkaline phosphatase were detected utilizing Fast Red (Vector, Cheminkpress, Craiova, Romania). The slides were counterstained with Mayer hematoxylin (Dako). Negative controls were obtained by omitting the primary antibodies.

Fluorescent double immunohistochemistry

After antigen retrieval and blocking steps, the sections were incubated with the first primary antibody anti-CD31 diluted 1:50 at 4°C overnight and then amplified by a 1 h incubation with a biotinylated goat anti-rabbit secondary (Dako) diluted at 1:200; biotin was detected with streptavidin-Texas Red (PerkinElmer,

Table 1. Association between D2-40 expression and clinico-pathological parameters.

Clinicopathological characteristics		No. of patients (%)	Podoplanin expression		
			Negative	Positive	
Gender	Male	29 (72.5)	16 (55.17)	13 (44.83)	
	Female	11 (27.5)	6 (54.54)	5 (45.46)	
Age	<65 years of age	15 (37.5)	9 (60)	6 (40)	
	>65 years of age	25 (62.5)	13 (52)	12 (48)	
Topography	Lips	21 (52.5)	9 (42.86)	12 (57.14)	
	Tongue	14 (35)	9 (64.29)	5 (35.61)	
	Other localizations	5 (12.5)	4 (80)	1 (20)	
Associated lesions	Hyperplasia	15 (37.5)	9 (60)	6 (40)	
	Dysplasia	Mild	10 (25)	6 (60)	4 (40)
		Moderate	5 (12.5)	3 (60)	2 (40)
		Severe	1 (2.5)	0	1 (100)
	Normal epithelium	9 (22.5)	4 (44.45)	5 (55.55)	

D2-40 expression in oral mucosa

Cheminkpress, Craiova, Romania) diluted 1:300 and incubated for 1 h at room temperature. After unspecific blocking with 2% BSA in PBS, the sections were incubated with the second primary antibody anti-D2-40 at a 1:100 dilution at 4°C overnight, followed by signal development using Alexa 488 labeled goat-anti-mouse antibody (Invitrogen, Cheminkpress, Craiova, Romania), diluted 1:200 at room temperature for 2 h. Antibody dilutions were made in 1% bovine serum albumin and 0.05% Tween. The same protocol was applied for the D2-40/Ki-67 (diluted 1:50) double staining. Signals were detected utilizing Alexa 488 labeled goat-anti-mouse and Alexa 594 labeled goat-anti-rabbit antibodies. The sections were counterstained with DAPI for 10 min and coverslipped with anti-fade mounting medium (Invitrogen).

Sections were examined and images captured at 10x, 20x, 40x and 60x magnification on a Nikon Eclipse 90i microscope (Nikon, Apidrag, Bucharest) equipped with a 5-megapixel cooled CCD camera and with narrow-band fluorescent filters centered for Alexa-594, -488 and DAPI excitation and emission wave-lengths. Images were acquired utilizing a Nikon frame grabber and the Nikon NIS-Elements software by three blinded observers (MC, PD, SA).

Morphometric analysis of lymphatic vascular area

The expression of D2-40 was assessed by calculating the total integrated optical density (IOD). Briefly, after the camera and the white and black intensity levels were calibrated, from each captured image the mask corresponding to the Hue/Saturation/Intensity (HSI) profile of the immunostaining was extracted. Total relative areas occupied by lymphatic vessels were calculated by means of the Image-Pro Plus software (Media Cybernetics, Inc., Bethesda, MD).

The proliferating lymphatic endothelial cell index (PLECI) was calculated as the percentage of the Ki-67-positive/ D2-40-positive lymphatic vessels from all the D2-40-positive lymphatic vessels observed on randomly selected microscopic fields. PLECI was calculated for each case analyzed, and then the results were averaged having common pathology as the denominator.

Fractal analysis

The fractal dimension (FD) of the lymphatic and blood vasculature was evaluated in normal oral mucosa. To this purpose, 20 images for each tumor-free resection margin area were acquired and the images coming from neighboring areas were merged in Adobe Photoshop (Adobe Systems Inc., San Jose, CA). Background staining, artifacts, or empty space were excluded. The layers corresponding to lymphatic and blood vasculature were imported in NIS-Elements software and further processed for areas and FD measurements. An RGB profile of the immunohistochemical signal was created and then applied for each layer to create binary signal

masks (Streptavidin-Texas Red for CD31 and Alexa 488 for D2-40A) utilizing the NIS-Elements software. The binary images were further processed in order to delineate the contours of the masks or to reduce the images to the skeleton of the vasculature. In both cases, a perimeter stepping algorithm was next used to calculate the FD of the contour, and respectively of the branching degree for each of the binary images (contour FD and pruning FD) (Fig. 1). All processing and fractal analyses were done by utilizing Image-Pro Plus software.

Statistical analysis

Data were expressed as mean \pm SEM. Values from groups were compared by using the paired Student t test. One-way ANOVA was used to test for differences among more than two independent groups, and correlations were analyzed by Pearson's test. Significance was defined as a P value < 0.05.

Results

Podoplanin expression in oral mucosa

Normal overlying epithelium was negative to D2-40. In tumor-free resection margins associated with hyperplasia and dysplasia an inconstant and heterogeneous D2-40 expression was observed in the basal layer of the overlying epithelium in the cytoplasm and in the plasma membrane (Fig. 2a,b).

D2-40 immunostaining was detected mostly in the epithelium of dysplastic lesions. A peculiar D2-40 expression was identified in tumor-free resection margins of lip tumors, where positive staining was constantly observed, with a focal pattern, particularly in the in basal layer cells of the lower lip.

Moreover, a strong podoplanin expression was detectable in the skin appendages of the OSCCs developed from lips. A strong ectoplasmic and membranous D2-40 staining of the basophilic germinative cells from the outer layer of normal sebaceous glands was detectable and immunoreactivity was also intense in the basal layer of the outer root sheets of human hair follicles, including the bulge area (Fig. 2c).

A variable D2-40 staining was observed in the myoepithelial cells of acini and ducts of minor salivary glands of tumor-free resection margins (Fig. 2d). Other immunoreactive structures were the perimysium of the skeletal muscle fibers and the perineurium of the nerve fibers. Finally, D2-40 staining was noticed in lymphatic endothelial cells and in the stromal reticular cells and follicular dendritic cells of the follicular germinal centers.

Regardless of the topography, in normal oral mucosa the lymphatic vessels were observed either close to the epithelium basal membrane, where they were less numerous, of small caliber and partially or fully

collapsed (Fig. 2e), and in the deep lamina propria, or annexed to the pilosebaceous follicles in the lips, minor salivary glands, nerves, skeletal muscle and lymphocytic infiltrates with lymphoid follicle formation, where they were more numerous, with larger caliber, either wide open or partially collapsed.

In dysplastic lesions the vessels were more numerous, with complex morphology, partially or fully collapsed and more close to the epithelium basal membrane (Fig. 2f). Their number was increased in the areas of lamina propria with abundant inflammatory infiltrate.

Morphometric analysis of lymphatic vascular area

Lymphatic relative vascular area overlapped in normal tongue ($0.52\pm 0.22\%$) and in the inferior lip

($0.58\pm 0.26\%$), whereas in oral floor had significantly lower values ($0.21\pm 0.18\%$) ($P = 0.032$) (Fig. 3a). In the tongue and in the lower lip, the lymphatic vascular areas showed a significant increase for tumoral specimens. Thus, these relative areas were $4.35\pm 1.39\%$ and $4.59\pm 1.26\%$ for tumor – tongue and tumor – lip specimens, as compared to normal – tongue ($0.52\pm 0.22\%$) and normal – lip ($0.58\pm 0.26\%$) oral epithelium, and dysplastic specimens ($1.87\pm 0.72\%$ for the tongue and respectively $1.90\pm 0.81\%$ for the lip) (one-way between types ANOVA, $F(2,24) = 4.32$, $p < 0.05$ (Fig. 3b,c). The differences between dysplastic lesions were not significant (Fig. 3d).

Total IOD expression was significantly higher in the normal lower lip ($3.6 \times 10^5 \pm 7.8 \times 10^4$) as compared to the tongue ($2.2 \times 10^5 \pm 6.2 \times 10^4$) ($P < 0.001$). No other intra-pathological difference could be observed between

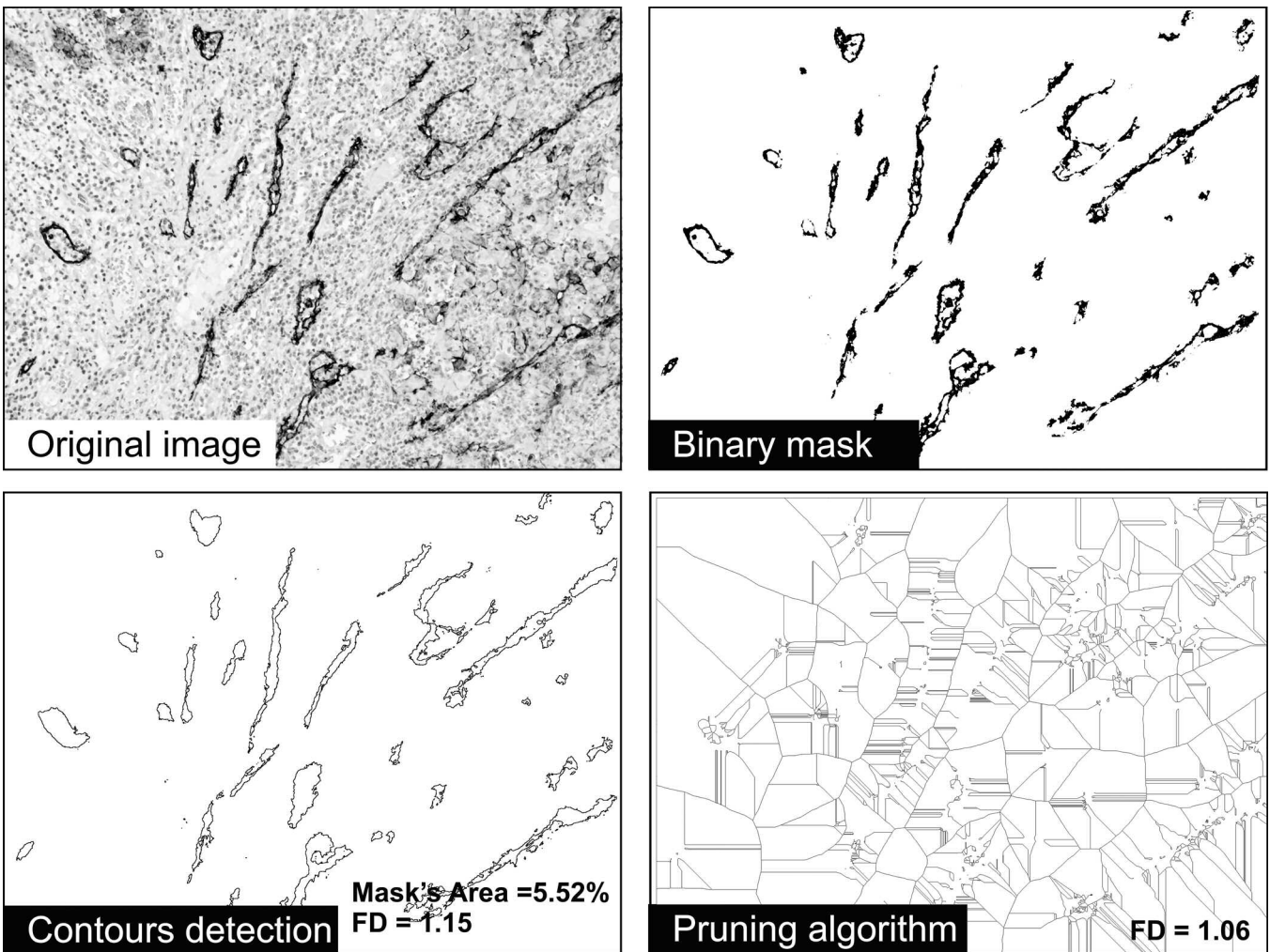


Fig. 1. Algorithms utilized to calculate the fractal dimension. The original image is first segmented into the binary mask of the immunohistochemical signal. Two algorithms are next employed to generate the contours of the binary objects (contour algorithm) and the dilation skeleton of the binary image (pruning algorithm). These pictures are used to calculate the complexity of the lymph vessel architecture by the perimeter stepping method.

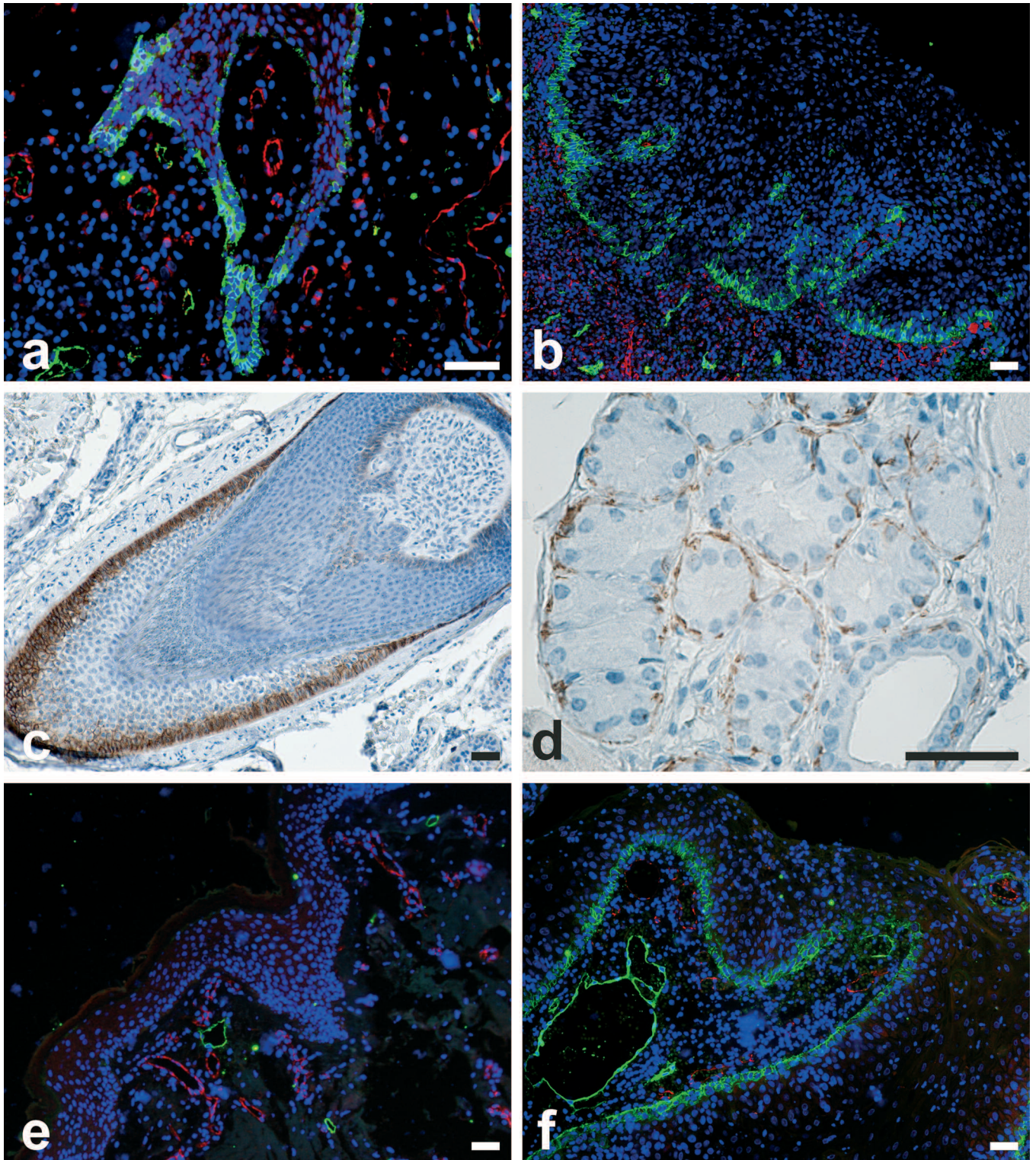


Fig. 2. Double (a, b, e, f), by using a monoclonal antibody anti-D2-40 (in green) and a polyclonal antibody anti-CD31 (in red), and single (c, d), by using a monoclonal antibody anti-D2-40, immunohistochemical staining of podoplanin expression in oral mucosa. **a.** Oral floor mucosa with hyperplasia. **b.** Tongue, mild to moderate dysplasia. **c.** Basal layer of the outer sheath of the root of human hair follicles. **d.** Myoepithelial cells of acini and ducts in minor salivary glands. **e.** Normal lower lip. **f.** Lower lip with simple dysplasia. Bars: 50 μ m.

preneoplastic and tumor tissue. These values differentiate between the normal, preneoplastic and neoplastic lesions in both the anatomical sites (one-way between types ANOVA, $F(3,28) = 4.04, p < 0.05$) (Fig. 4).

In the tumor free resection margins associated with normal tissue, lymphatic vessels were negative for Ki-67 (the PLECI was under 5%). In tumor free resection margins associated with preneoplastic lesions, active proliferating lymph vessels were identified; in fact, the value of PLECI was higher in the dysplastic lesions (23%) as compared to hyperplastic lesions (20%). These vessels showed mitotic figures (Fig. 4). In the tumors corresponding to the free resection margins associated with preneoplastic lesions, PLECI index increased at least two to three times. Overall, PLECI could differentiate between normal, preneoplastic and, tumor tissues (one-way between types ANOVA, $F(2,19) = 4.94, p < 0.05$). Also PLECI revealed a good direct correlation with the total D2-40 expression's IOD values, ($r=0.654, n=24, p=0.002$) and with the relative

lymph vessel areas ($r=0.544, n=25, p=0.008$).

Fractal lymphatic vessels analysis

Contour FD values were significantly lower in the lower lip (1.11 ± 0.04), as compared to tongue (1.15 ± 0.06) and to oral floor mucosa (1.20 ± 0.07) ($P=0.012$) (Fig. 3a), whereas pruning FD values showed no significant differences ($P > 0.05$).

In the tongue, contour FD values were significantly lower in normal (1.15 ± 0.06) as compared to tumoral tissue (1.22 ± 0.02) ($P=0.003$), whereas no significant differences were recognizable as compared to dysplastic lesions ($P > 0.05$) (Fig. 3b).

In the lower lip, contour FD values were significantly lower in normal (1.11 ± 0.04) as compared to dysplastic and tumoral tissue (1.20 ± 0.06 and, respectively, 1.23 ± 0.02), but the differences were not statistically significant ($P > 0.05$) (Fig. 3c).

When grouping all tissues harboring a dysplastic

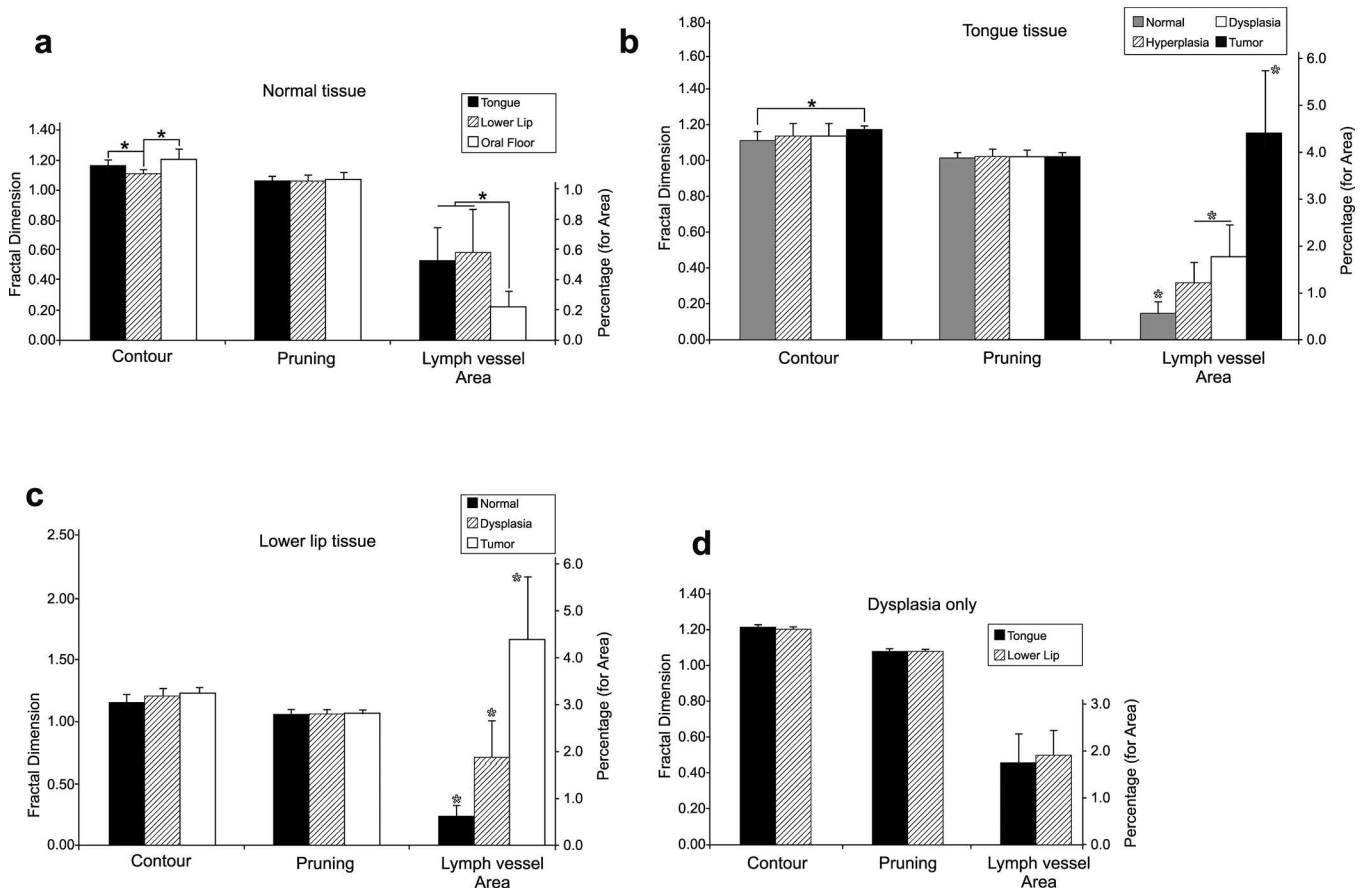


Fig. 3. Fractal analysis. Contour and pruning fractal dimension and percentage of lymphatic vessel areas: evaluated in normal tissue in tongue, lower lip and oral floor (a); evaluated in normal, hyperplastic and dysplastic tongue tissue (b); evaluated in normal and dysplastic lower lip tissue (c); compared in tongue and lower lip dysplastic tissue lesions (d). Full stars illustrate significant differences on t tests, and empty stars show significance on ANOVA testing; $P < 0.05$. Error bars represent SEM.

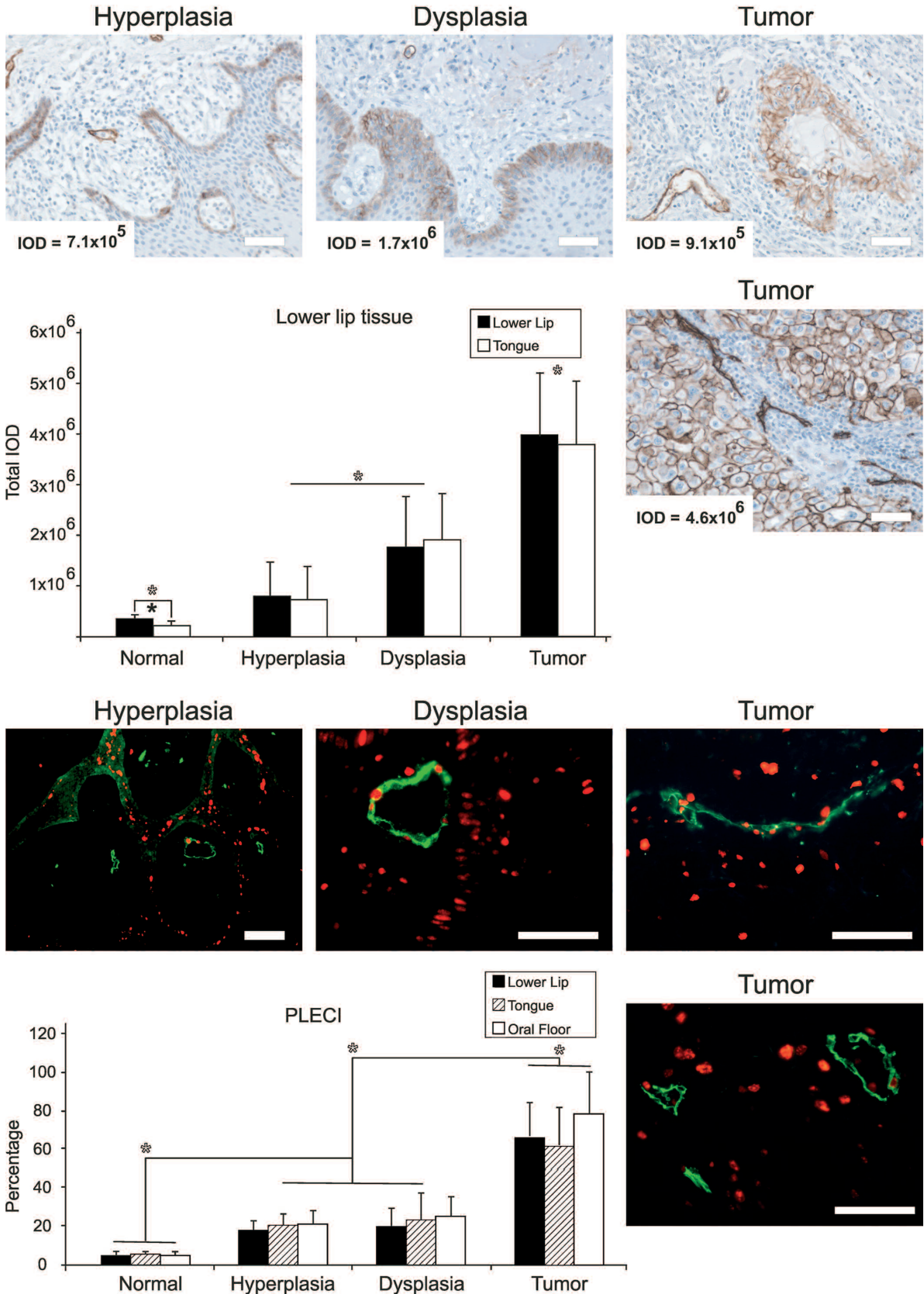
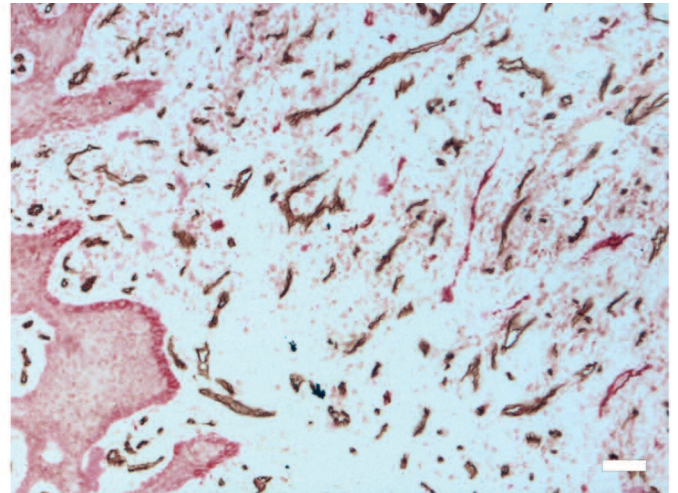
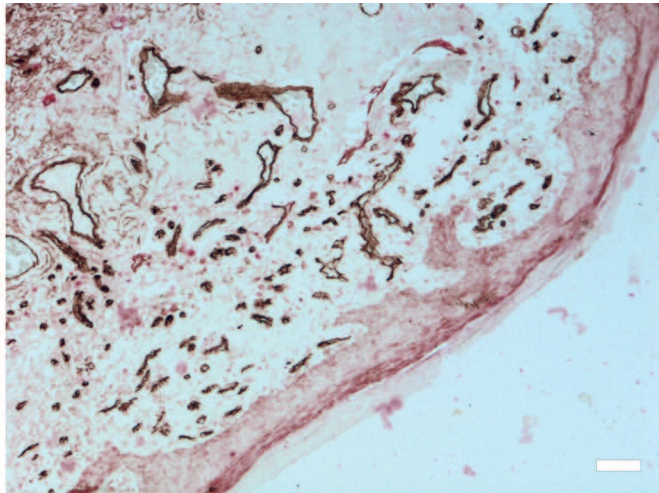


Fig. 4. Upper panel. Total IOD values in normal, hyperplastic, dysplastic and tumoral tissues at the level of the lower lip and tongue; full stars indicate significant differences on t tests, and empty stars on ANOVA testing; $P < 0.05$. Error bars represent SEM. In this panel representative immunohistochemical pictures obtained by using the anti-D2-40 antibody and the corresponding values are appreciable. **Lower panel.** Proliferative Lymphatic Endothelial Cell Index (PLECI) values in normal, hyperplastic, dysplastic and tumoral tissue at the level of the lower lip, tongue and oral floor tissue; empty stars show significance on ANOVA testing; $P < 0.05$. In this panel representative immunohistochemical pictures obtained by a double staining with the anti-D2-40 antibody (green) and anti-Ki67 antibody (red) are appreciable. Bars: 50 μm .

lesion, contour FD and pruning FD could not differentiate between tongue and lower lip tissues (Fig. 3d).

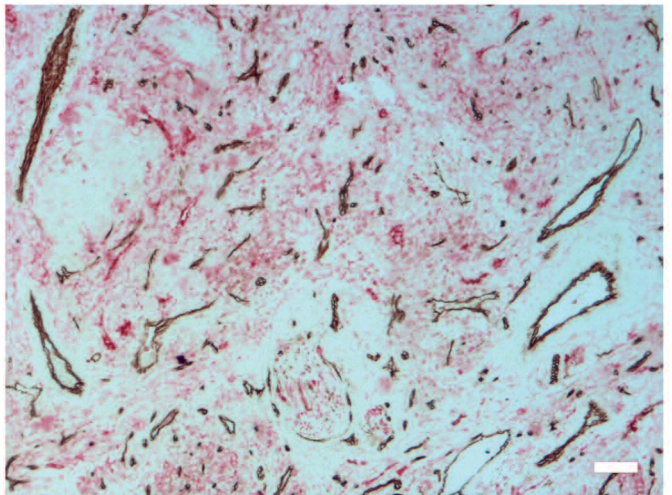
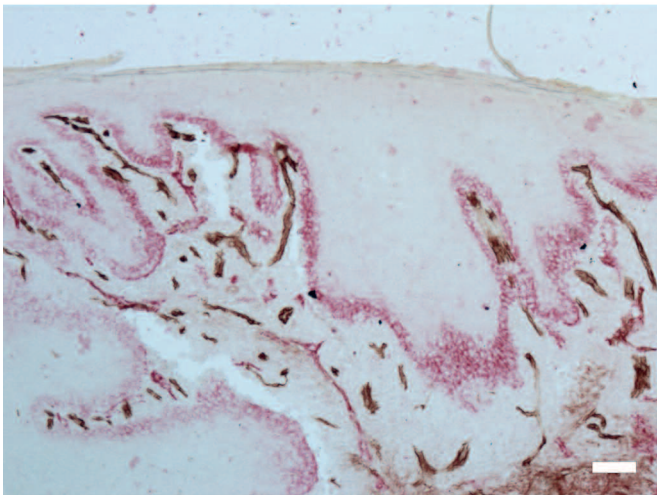
When applying the same algorithms to the blood vessels, resulting FD values tended to be higher as compared to the lymphatic FD values, but the



Normal

Hyperplasia

	Lymph Vessels	Blood Vessels	Lymph Vessels	Blood Vessels
Contour FD	1.14	1.16	1.15	1.18
Pruning FD	1.06	1.08	1.06	1.07
Area	0.52%	6.75%	0.86%	5.05%



Dysplasia

Tumor

	Lymph Vessels	Blood Vessels	Lymph Vessels	Blood Vessels
Contour FD	1.17	1.19	1.18	1.21
Pruning FD	1.08	1.10	1.08	1.08
Area	2.30	9.98%	2.23%	6.35%

Fig. 5. Double immunostaining (D2-40 – red/ CD31-brown) shows the contour and pruning fractal values together with the relative vessel areas in normal, hyperplastic dysplastic and tumor tissues. Bars: 50 μm.

differences were not significant (Fig. 5).

Discussion

Podoplanin expression in oral mucosa

The results of the present study indicate the absence of podoplanin expression in normal epithelium of oral mucosa with the exception of OSCCs developed in the lower lip tissue. Podoplanin expression is variable in tumor-free resection margins associated with hyperplastic or dysplastic lesions.

PA2.26 antigen, a homolog of human podoplanin, was not detectable in the normal oral epithelium and in premalignant lesions with moderate to intense dysplasia (Martin-Villar et al., 2005). However, a positive staining was recognizable in the reactive mucosa adjacent to OSCCs, regardless of PA2.26 reactivity of tumoral cells, and the same authors observed that the PA2.26 expression was restricted to basal-like cells in the hyperplastic mucosa and no reactivity was noted in the upper layers. Yuan et al. demonstrated that podoplanin is not detectable in normal squamous epithelium adjacent to the tumors, or its expression is low in basal cells, whereas a high expression was observed in some hyperplastic and dysplastic epithelial areas adjacent to the tumors (Yuan et al., 2006). More recently, Kawaguchi et al. showed that in more than 37% of patients with oral leukoplakia podoplanin was expressed in the basal and upper layers, and they found that podoplanin expression increases with increased severity of dysplasia, from mild dysplasia to moderate or severe dysplasia/carcinoma in situ (Kawaguchi et al., 2008). In this context, the clonal expansion of the podoplanin-expressing cells in the epithelial layers supports tumorigenesis.

Podoplanin expression was also noticed in the basal cells of other stratified epithelia: Schacht et al. demonstrated a focal podoplanin expression in basal epithelial cells of the skin, cervix and esophagus (Schacht et al., 2005); Gomaa et al. noticed a focal staining of the basal layer of the epidermis in several facial specimens (Gomaa et al., 2007). Basal cells of benign cervical squamous epithelia express a strong D2-40 immunoreactivity, confined to the lower third of the epithelium squamous cell carcinomas in situ (Dumoff et al., 2005). In uterine cervix the frequency of D2-40 immunoreactivity decreased towards malignancy (Longatto-Filho et al., 2007).

Our study showed that D2-40 immunoreactivity is strongly detectable in the basal layer of the skin appendages in OSCCs cases in lips, according to the findings reported by other authors (Schacht et al., 2005; Gomaa et al., 2007; Liang et al., 2007). This observation that some of the basal cells from the lower lip epithelium of the tumor-free resection margins are positive for D2-40 could be related to the presence at this level of the reserve cells or stem cells. Their number was increased in the proximity of the tumor area, meaning that some of

these cells could progress to malignant transformation. D2-40 expression in tumor-free resection margins could be used as a prognostic factor for the development of recurrences or other primary metachrone tumors. Accordingly, Atsumi et al. proved that podoplanin is a novel marker for enrichment in tumor-initiating cells with stem-cell-like properties (Atsumi et al., 2008).

Schacht et al. demonstrated a strong podoplanin expression in myoepithelial cells of the breast glands and of salivary glands, in myofibroblasts of the prostate, fibromyocytes of the testis, and cells of the perineurium (Schacht et al., 2005). Hata et al. showed a strong reactivity to podoplanin in myoepithelial cells from mouse salivary glands (Hata et al., 2008). It was hypothesized that accordingly to its contractile function, podoplanin might play an important role in mediating cellular contractile properties and cytoskeletal reorganization.

Morphometric analysis of lymphatic vascular area

We noticed the existence of a lymphatic network beneath the underlying oral epithelium consisting in small, irregularly shaped, thin walled and generally partially or fully collapsed vessels, according to the observations of Muñoz-Guerra et al. in the surgical tissue samples of 61 patients with early-stage (Stages I–II) oral carcinoma (Munoz-Guerra et al., 2004).

Morphometric analysis has indicated that lymphatic vascular area increases progressively from normal tissue to precancerous lesions and, respectively, tumor tissue. PLECI reflects the gradual progression from normal towards tumoral tissue, expressed by a good direct correlation with the total IOD values; but without a clear-cut distinction between hyperplastic and dysplastic lesions.

In the last decade there have been several attempts to describe the lymphatic architecture in the oral mucosa. Liang et al. examined the lymphatic architecture in the lingual mucosal epithelium in the golden hamster and observed that in the lamina propria at the lingual dorsum there are irregular networks of lymphatic capillaries from which blind end lymphatic capillaries extend into the connective tissue papilla (Liang and Fujimura, 2000). In contrast, a hexagonal network of lymphatic capillaries was noticed under the flattened basal layer of the sublingual epithelium, with no blind end lymphatic capillaries and responsible for absorption at the sublingual surface. Fujimura et al. investigated the lymphatic architecture beneath the oral mucosa using enzyme histochemical staining and serial section 3D reconstructions (Fujimura et al., 2007). They demonstrated that the lymphatic network beneath the oral mucosa ran like a network of rivers beneath the mucosal epithelium in which the lymph constantly flowed from narrow into wider lymphatic vessels without stagnation. From this network blind-end capillaries detach and enter into the papilla propria at the level of the first molar area, where they acquire a

glomerulus-like structure. Such glomerular structures are more efficient in absorption compared to simple blind-end tubular structures reported in tongue oral region (Chen and Fujimura, 1994; Liang and Fujimura, 2000; Fujimura and Nozaka, 2002; Fujimura et al., 2003).

In this study, for the first time we have demonstrated that lymphangiogenesis occurs at the resection margins of OSCCs not invaded by the tumor cells. In this place, PLECI progressively increased from normal tissue to dysplastic lesions and, respectively, tumor tissue.

Our data agree with previously published reports indicating that lymphangiogenesis is an active process occurring during tumor progression in head and neck squamous cell carcinoma (Beasley et al., 2002) and is correlated with metastatic process and clinical outcome (Kyzas et al., 2005; Zhao et al., 2008).

Fractal lymphatic vessels analysis

In this study, for the first time, the lymphatic vasculature at the level of the oral mucosa has been examined by utilizing FD analysis in a comparative study of the normal, hyperplastic and dysplastic resection borders, and revealed a significant difference only for the contour FD denominator, particularly at the level of the tongue.

Both contour and pruning FD values were close to unity, and these data might be explained by the particular morphology of the lymphatic vessels which are known to be smoother and more unbranched as compared to the blood vessels. Nevertheless, these values revealed significant differences between normal, preneoplastic and tumoral tissues.

De Felice et al. observed geometric pattern abnormalities in the oral mucosa of patients with hereditary non-polyposis colorectal cancer syndrome, consisting of increased vessel density and presence of multiple vascular loops (De Felice et al., 2003). The same authors proved that in Ehlers-Danlos syndrome there is an abnormal oral vascular network geometric complexity consisting of increased trajectories' density, decreased vessel tortuosity and generalized small loops features (De Felice et al., 2004). Landini and Rippin showed that epithelial changes occurring in severe dysplasia and invasive carcinoma were followed by an increase in fractal blood vessel dimension in invasive carcinoma as compared to normal epithelium, and established an accuracy of 85% for diagnosis using fractal analysis of the epithelial-connective tissue interface in specimens of epithelial dysplasia and squamous cell carcinoma of the floor of the mouth (Landini and Rippin, 1993, 1996). Finally, using fractal geometry Abu and Landini proved that the complexity of the epithelial-connective tissue interface was significantly increased from normal through premalignant to malignant oral mucosal lesions (Abu and Landini, 2003). More recently, Goutzanis et al., comparing the blood vascular fractal dimension from oral carcinomas versus oral non-neoplastic lesions,

demonstrated that the value of this parameter was significantly higher in tumoral lesions (Goutzanis et al., 2009).

Overall, our study indicates that podoplanin expression in oral epithelium is an early event in tumorigenesis and predicts the evolution of preneoplastic lesions, and the evaluation of D2-40 expression in tumor-free resection margins could predict the potential of recurrences in oral cancer. Moreover, an increase of the area occupied by lymphatic vessels in pre-malignant and malignant oral mucosal lesions could be another reliable prognostic factor in such lesions.

Acknowledgements. The present work was partially supported from the Romanian founding grant CNCSIS ID155.

References

- Abu E.R. and Landini G. (2003). Quantification of the global and local complexity of the epithelial-connective tissue interface of normal, dysplastic, and neoplastic oral mucosae using digital imaging. *Pathol. Res. Pract.* 199, 475-482.
- Atsumi N., Ishii G., Kojima M., Sanada M., Fujii S. and Ochiai A. (2008). Podoplanin, a novel marker of tumor-initiating cells in human squamous cell carcinoma A431. *Biochem. Biophys. Res. Commun.* 373, 36-41.
- Beasley N.J., Prevo R., Banerji S., Leek R.D., Moore J., van T.P., Cox G., Harris A.L. and Jackson D.G. (2002). Intratumoral lymphangiogenesis and lymph node metastasis in head and neck cancer. *Cancer Res.* 62, 1315-1320.
- Breiteneder-Geleff S., Soleiman A., Kowalski H., Horvat R., Amann G., Kriehuber E., Diem K., Weninger W., Tschachler E., Alitalo K. and Kerjaschki D. (1999). Angiosarcomas express mixed endothelial phenotypes of blood and lymphatic capillaries: podoplanin as a specific marker for lymphatic endothelium. *Am. J. Pathol.* 154, 385-394.
- Chen K.H. and Fujimura A. (1994). Distribution of the lymphatic vessels in golden hamster tongue. *Dent. J. Iwate Med. Univ.* 19, 91-102.
- De Felice C., Latini G., Bianciardi G., Parrini S., Fadda G.M., Marini M., Laurini R.N. and Kopotic R.J. (2003). Abnormal vascular network complexity: a new phenotypic marker in hereditary non-polyposis colorectal cancer syndrome. *Gut* 52, 1764-1767.
- De Felice C., Bianciardi G., Dileo L., Latini G. and Parrini S. (2004). Abnormal oral vascular network geometric complexity in Ehlers-Danlos syndrome. *Oral Surg. Oral Med. Oral Pathol. Oral Radiol. Endod.* 98, 429-434.
- Dumoff K.L., Chu C., Xu X., Pasha T., Zhang P.J. and Acs G. (2005). Low D2-40 immunoreactivity correlates with lymphatic invasion and nodal metastasis in early-stage squamous cell carcinoma of the uterine cervix. *Mod. Pathol.* 18, 97-104.
- Fujimura A. and Nozaka Y. (2002). Analysis of the three-dimensional lymphatic architecture of the periodontal tissue using a new 3D reconstruction method. *Microsc. Res. Tech.* 56, 60-65.
- Fujimura A., Sato Y., Shoji M., Onodera M. and Nozaka Y. (2007). Lymphatic architecture of the oral region: beneath the buccal mucosa. *Microvasc. Res. Commun.* 1, 9-11.
- Fujimura A., Seki S., Liao M.Y., Hu X., Onodera M. and Nozaka Y. (2003). Three dimensional architecture of lymphatic vessels in the

D2-40 expression in oral mucosa

- tongue. *Lymphology* 36, 120-127.
- Gandarillas A., Scholl F.G., Benito N., Gamallo C. and Quintanilla M. (1997). Induction of PA2.26, a cell-surface antigen expressed by active fibroblasts, in mouse epidermal keratinocytes during carcinogenesis. *Mol. Carcinog.* 20, 10-18.
- Gomaa A.H., Yaar M. and Bhawan J. (2007). Cutaneous immunoreactivity of D2-40 antibody beyond the lymphatics. *Am. J. Dermatopathol.* 29, 18-21.
- Goutzani L.P., Papadogeorgakis N., Pavlopoulos P.M., Petsinis V., Plochoras I., Eleftheriadis E., Pantelidaki A., Patsouris E. and Alexandridis C. (2009). Vascular fractal dimension and total vascular area in the study of oral cancer. *Head Neck* 31, 298-307.
- Hata M., Ueki T., Sato A., Kojima H. and Sawa Y. (2008). Expression of podoplanin in the mouse salivary glands. *Arch. Oral Biol.* 53, 835-841.
- Hong Y.K., Harvey N., Noh Y.H., Schacht V., Hirakawa S., Detmar M. and Oliver G. (2002). Prox1 is a master control gene in the program specifying lymphatic endothelial cell fate. *Dev. Dyn.* 225, 351-357.
- Hunyady B., Krempels K., Harta G. and Mezey E. (1996). Immunohistochemical signal amplification by catalyzed reporter deposition and its application in double immunostaining. *J. Histochem. Cytochem.* 44, 1353-1362.
- Kaneko M.K., Kato Y., Kitano T. and Osawa M. (2006). Conservation of a platelet activating domain of Aggrus/podoplanin as a platelet aggregation-inducing factor. *Gene* 378, 52-57.
- Kawaguchi H., El-Naggar A.K., Papadimitrakopoulou V., Ren H., Fan Y.H., Feng L., Lee J.J., Kim E., Hong W.K., Lippman S.M. and Mao L. (2008). Podoplanin: a novel marker for oral cancer risk in patients with oral premalignancy. *J. Clin. Oncol.* 26, 354-360.
- Kyzas P.A., Geleff S., Batistatou A., Agnantis N.J. and Stefanou D. (2005). Evidence for lymphangiogenesis and its prognostic implications in head and neck squamous cell carcinoma. *J. Pathol.* 206, 170-177.
- Landini G. and Rippin J.W. (1993). Fractal dimensions of the epithelial-connective tissue interfaces in premalignant and malignant epithelial lesions of the floor of the mouth. *Anal. Quant. Cytol. Histol.* 15, 144-149.
- Landini G. and Rippin J.W. (1996). How important is tumour shape? Quantification of the epithelial-connective tissue interface in oral lesions using local connected fractal dimension analysis. *J. Pathol.* 179, 210-217.
- Liang H., Wu H., Giorgadze T.A., Sariya D., Bellucci K.S., Veerappan R., Liegl B., Acs G., Elenitsas R., Shukla S., Youngberg G.A., Coogan P.S., Pasha T., Zhang P.J. and Xu X. (2007). Podoplanin is a highly sensitive and specific marker to distinguish primary skin adnexal carcinomas from adenocarcinomas metastatic to skin. *Am. J. Surg. Pathol.* 31, 304-310.
- Liang J.C. and Fujimura A. (2000). Lymphatic architecture beneath the mucosal membrane of the tongue. *Dent. J. Iwate Med. Univ.* 25, 283-291.
- Longatto-Filho A., Pinheiro C., Pereira S.M., Etlinger D., Moreira M.A., Jube L.F., Queiroz G.S., Baltazar F. and Schmitt F.C. (2007). Lymphatic vessel density and epithelial D2-40 immunoreactivity in pre-invasive and invasive lesions of the uterine cervix. *Gynecol. Oncol.* 107, 45-51.
- Martin-Villar E., Scholl F.G., Gamallo C., Yurrita M.M., Munoz-Guerra M., Cruces J. and Quintanilla M. (2005). Characterization of human PA2.26 antigen (T1alpha-2, podoplanin), a small membrane mucin induced in oral squamous cell carcinomas. *Int. J. Cancer* 113, 899-910.
- Martin-Villar E., Megias D., Castel S., Yurrita M.M., Vilaro S. and Quintanilla M. (2006). Podoplanin binds ERM proteins to activate RhoA and promote epithelial-mesenchymal transition. *J. Cell Sci.* 119, 4541-4553.
- Munoz-Guerra M.F., Marazuela E.G., Martin-Villar E., Quintanilla M. and Gamallo C. (2004). Prognostic significance of intratumoral lymphangiogenesis in squamous cell carcinoma of the oral cavity. *Cancer* 100, 553-560.
- Nose K., Saito H. and Kuroki T. (1990). Isolation of a gene sequence induced later by tumor-promoting 12-O-tetradecanoylphorbol-13-acetate in mouse osteoblastic cells (MC3T3-E1) and expressed constitutively in ras-transformed cells. *Cell Growth Differ.* 1, 511-518.
- Ordonez N.G. (2006). Podoplanin: a novel diagnostic immunohistochemical marker. *Adv. Anat. Pathol.* 13, 83-88.
- Rishi A.K., Joyce-Brady M., Fisher J., Dobbs L.G., Floros J., VanderSpek J., Brody J.S. and Williams M.C. (1995). Cloning, characterization, and development expression of a rat lung alveolar type I cell gene in embryonic endodermal and neural derivatives. *Dev. Biol.* 167, 294-306.
- Schacht V., Dadras S.S., Johnson L.A., Jackson D.G., Hong Y.K. and Detmar M. (2005). Up-regulation of the lymphatic marker podoplanin, a mucin-type transmembrane glycoprotein, in human squamous cell carcinomas and germ cell tumors. *Am. J. Pathol.* 166, 913-921.
- Wicki A. and Christofori G. (2007). The potential role of podoplanin in tumour invasion. *Br. J. Cancer* 96, 1-5.
- Wicki A., Lehenbre F., Wick N., Hantusch B., Kerjaschki D. and Christofori G. (2006). Tumor invasion in the absence of epithelial-mesenchymal transition: podoplanin-mediated remodeling of the actin cytoskeleton. *Cancer Cell* 9, 261-272.
- Yuan P., Temam S., El-Naggar A., Zhou X., Liu D.D., Lee J.J. and Mao L. (2006). Overexpression of podoplanin in oral cancer and its association with poor clinical outcome. *Cancer* 107, 563-569.
- Zhao D., Pan J., Li X.Q., Wang X.Y., Tang C. and Xuan M. (2008). Intratumoral lymphangiogenesis in oral squamous cell carcinoma and its clinicopathological significance. *J. Oral Pathol. Med.* 37, 616-625.